Principles of Solid Rocket Motor Design

Naminosuke Kubota
Scientific Advisor, Mitsubishi Electric Corporation, Kamimachiya 325, Kamakura 247-0065, Japan
email: Naminosuke.Kubota@kama.melco.co.jp

ABSTRACT

A number of parameters are needed to design a rocket motor to satisfy the specified flight trajectory of its payload. The major components of a rocket motor are propellant grain, motor case and its insulation, nozzle, and igniter. One of the key parameters is the burn rate characteristic of the propellant grain that is set in a rocket chamber either by cast method or by free-stand. The combustion phenomena in the motor are highly dependent on the design of the perforated propellant grains in which transient burning, erosive burning, oscillatory burning, and unstable burning occur. As a special rocket motor design, a two stage motor with two propellant grains in a single chamber, is described and compared with practical firing test results.

Keywords: flight dynamics, rocket motor, propellant combustion, two-stage motor, igniter, propellant grain, nozzle

1. Introduction

Rocket projectiles are used to carry a payload from a launch site to a specified location or altitude within a specified time. Rocket motors are used to generate propulsive forces for the projectile flight of which velocity is either subsonic or supersonic, or even hypersonic. The size, mass, and thrust of solid rocket motors vary widely from the space shuttle booster (3.77 m in diameter, 45.45 m in length, 502.12×10^3 kg of mass, and 11.79 MN thrust at sea level) to a micro-rocket motor (smaller than 0.01 m in diameter, 0.05 m in length, 0.1 kg of mass, and 1.0 N thrust). However, the fundamental concepts of rocket motor design are independent of the size, mass, and thrust.

The thrust generated by the combustion of a solid propellant is determined not only by the chemical energy of the propellant but also the thermodynamic processes in a rocket motor. In this article, the physicochemical properties of propellants and the energy conversion processes in rocket motors are presented in light of the design of various types of rocket motors.

2. Flight Dynamics of Rocket Projectiles

2.1 Momentum Change of Exhaust Gas

The design of a rocket projectile assisted by a solid rocket motor is determined by the requirement of flight trajectory. Once its flight trajectory and payload are given, an optimized total mass of the projectile and the thrust versus time of flight are determined.[1] The flight path of the projectile is dependent on various external parameters such as gravitational force, air density, wind velocity, and so on.

Although the physical structure of solid rocket motors is a very simplified one when compared with that of liquid rocket motors, once the propellant is ignited, the thrust generated by the propellant combustion cannot be changed. Thus, the chosen design parameters are not flexible. The mass and the size of the propellant grain are evaluated through the required thrust versus burning time relationship. In general, as the mass of the payload increases, the mass of the propellant grain in the motor increases, and the size of the motor also increases.

The momentum change of the projectile during rocket motor operation is represented by

$$\left(M-\Delta m\right)\left(V+\Delta V\right)-MV=M\Delta V-V\Delta m \quad (1)$$

where M is the mass of the projectile at time t, V is the flight velocity, ΔV is the velocity change during the time interval Δt, Δm is the exhaust mass from the projectile during the time interval Δt. In equation 1, it is assumed that the $\Delta V \Delta m$ term is such a small value that it can be ignored. The momentum change of the exhaust gas is represented by

$$\left(V - u_e\right)\Delta m = V\Delta m - u_e \Delta m \tag{2}$$

where u_e is the exhaust gas velocity from the projectile. Thus, the overall momentum change is given as

$$M\Delta V - u_e \Delta m \tag{3}$$

The thrust F is given by the momentum changes of the projectile and the exhaust gas per unit time as

$$F = \frac{M\Delta V - u_e \Delta m}{\Delta t} \tag{4}$$

2.2 Aerodynamic Drag and Flight Trajectory

As shown in Figure 1, the force balance acting on the rocket projectile is represented by

$$F = -D - Mg\cos\theta \tag{5}$$

where D is the aerodynamic drag and g is the gravitational acceleration. Since the mass of the projectile decreases (ΔM during the time interval Δt), the relationship of $\Delta m/\Delta t = -(\Delta M/\Delta t)$ is obtained. Using equations 4 and 5, one gets the force balance of

$$M\Delta V + u_e \Delta M = \left(-D - Mg\cos\theta\right)\Delta t \tag{6}$$

Thus, the velocity increase of the projectile is obtained as

$$\Delta V = -\frac{u_e \Delta M}{M} - \frac{D\Delta t}{M} - g\cos\theta\Delta t \tag{7}$$

Assume horizontal flight ($\theta = 90°$), for example, without aerodynamic drag ($D = 0$), the flight velocity increases from V_0 to V and the mass decreases from M_0 to M. By integrating Equation 7, one gets

$$V - V_0 = u_e \ln\varphi \tag{8}$$

where φ is the mass ratio defined by $\varphi = M_0/M$. The maximum flight velocity V_{max} is obtained

$$V_{max} = V_0 + u_e \ln\varphi_0 \tag{9}$$

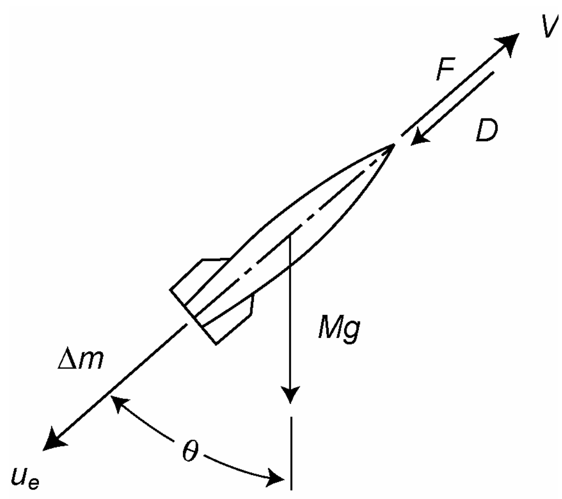

Figure 1. Force balance during flight of a rocket projectile.

where φ_0 is the mass ratio of the initial mass M_0 and the burnout mass M_b of the projectile.

In the case of vertical flight ($\theta = 0°$) from the ground without aerodynamic drag ($D = 0$), the flight velocity at time t is also obtained by the integration of equation 7 as

$$V = u_e \ln\varphi - gt \tag{10}$$

The altitude h_b at the burnout time t_b is obtained by the integration of equation 10 as

$$h_b = u_e t_b \left\{\frac{1 - \ln\varphi_0}{\varphi_0 - 1}\right\} - \frac{g t_b^2}{2} \tag{11}$$

It can be seen from equation 11 that the flight altitude increases as φ_0 increases and/or u_e increases. The maximum flight altitude h_f of the projectile is obtained by the conservation of the kinetic energy and the potential energy of the projectile as

$$M_b \frac{V_b^2}{2} = M_b g\left(h_f - h_b\right) \tag{12}$$

Since the burnout velocity V_b at time t_b is obtained by $V_b = u_e \ln\varphi_0 - g\,t_b$, h_f is obtained as

$$h_f = u_e^2 \frac{\left(\ln\varphi_0\right)^2}{2g} - u_e t_b \left(\frac{\varphi_0 \ln\varphi_0}{\varphi_0 - 1} - 1\right) \tag{13}$$

The thrust required for flight in the atmosphere is determined by the aerodynamic drag for deceleration shown in equation 5. The aerodynamic drag is represented by

$$D = \frac{1}{2} \rho_a V^2 A C_d \tag{14}$$

where V is flight velocity, A is the maximum cross sectional area of the projectile, ρ_a is air density, and C_d is the drag coefficient. Since C_d is dependent on the flight velocity and the physical shape of the projectile, C_d must be determined by either wind tunnel tests, mathematical computations using computational fluid dynamics (CFD), or physical simulations. Figure 2 shows a typical drag coefficient of a rocket projectile as a function of Mach number. Mach number is defined as the ratio of the flight velocity and the speed of sound in the flight atmosphere.

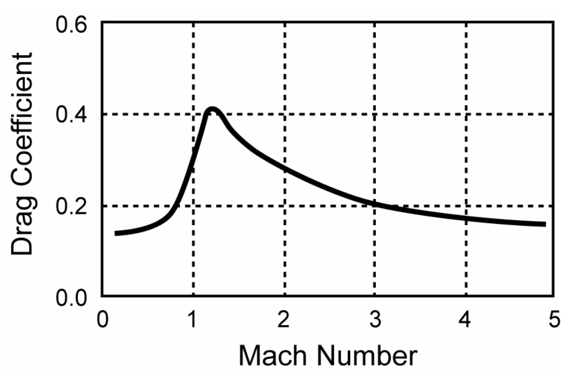

Figure 2. Drag coefficient of a typical rocket projectile as a function of Mach number.

The deceleration of the projectile after burnout (a) due to the aerodynamic drag and gravitational force is obtained by

$$a = \frac{F}{M} = -\frac{1}{2} C_d \rho_a A \frac{V^2}{M} - g \cos\theta \tag{15}$$

In the case of θ = constant, the velocity at time t is obtained by the integration of equation 15 as

$$V = V_b - \int \left(\frac{1}{2} C_d \rho_a A \frac{V^2}{M} \right) \mathrm{dt} - gt \cos\theta \tag{16}$$

The flight altitude at time t is obtained by the integration of equation 16. It must be noted that C_d is a function of velocity when equations 15 and 16 are integrated.

If one assumes that the flight is vertical and C_d remains constant during free flight, the altitude h_f is obtained by the integration of equation 16 as

$$h_f = \int V \, dt \tag{17}$$

Using equations 16 and 17, the relationship between V and h_f as a function of t is obtained.

3. Thermodynamics for Thrust Generation

3.1 Structure and Combustion of a Rocket Motor

The chemical energy of a solid propellant is converted to thrust that is generated by a rocket motor through combustion phenomena. When a solid propellant burns in a rocket motor, high temperature combustion products are formed and high pressure is created in the motor. Then the thrust is generated by the high pressure based on the momentum change through a thermodynamic nozzle attached at the aft end of the combustion chamber. Figure 3 shows the fundamental structure of a solid rocket motor. The motor consists of combustion chamber, nozzle, and propellant. The propellant grain is set in the combustion chamber and the nozzle is attached at the aft end of the combustion chamber. The nozzle is used as an accelerator of the combustion gas from subsonic flow to supersonic flow, and the combustion gas is exhausted to the atmosphere through the nozzle. The nozzle consists of a convergent part, a throat, and a divergent part. The convergent part accelerates the subsonic flow to sonic speed and then the divergent part accelerates the gas flow from sonic speed to supersonic speed. The maximum speed is obtained at the exit plane of the divergent part. The convergent part and the divergent part (A_e) are connected at the nozzle throat where the cross-sectional area is the minimum of the nozzle A_t.[1–3]

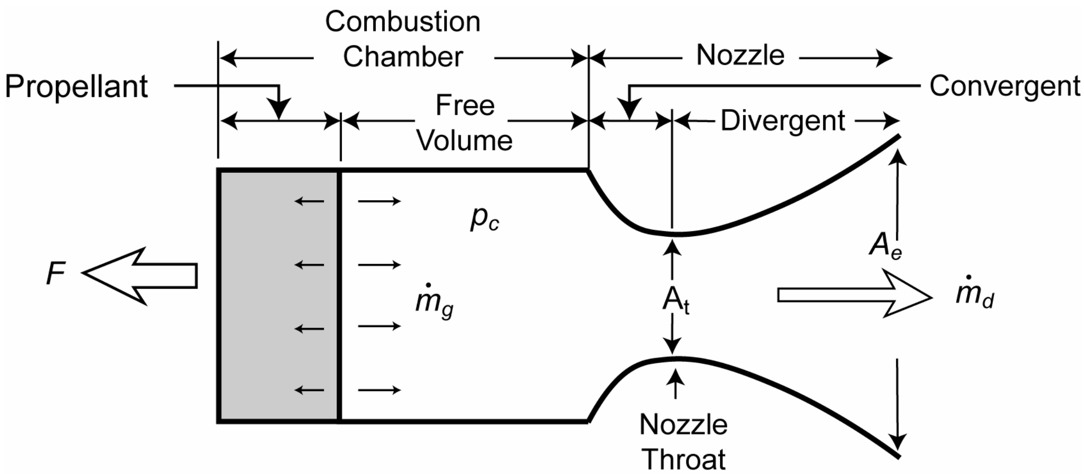

Figure 3. Structure of a rocket motor and burning of a propellant grain.

Since the propellant grain is set in the combustion chamber, the free volume in the chamber increases as the propellant grain is consumed. The internal surface of the chamber may 1be covered by an insulating material to protect the chamber wall from the high temperature combustion products. Thermally resistant material is used for the nozzle to prevent thermal erosion from the high temperature and high velocity gas flow. An igniter is attached to the chamber wall to ignite the initial surface of the propellant grain.

3.2 Mass Balance in a Rocket Motor

As shown in Figure 4, a rocket motor is a high pressure vessel in which high pressure is formed by the combustion of a propellant grain in the vessel. The high pressure decreases in the nozzle as the gas flow velocity increases. Since the pressure acts perpendicular to the internal surface of the combustion chamber and the nozzle, the resultant pressure acting on the rocket motor yield the thrust. Thus, the pressure in the chamber and in the nozzle is an important parameter in determining the thrust characteristics of the rocket motor.

When a propellant grain set in a combustion chamber burns, combustion gas is generated and is discharged from the nozzle as shown in Figure 3. The mass generation rate in the combustion chamber, $\dot{m}_g$, is given by

$$\dot{m}_g = \rho_p A_b r \tag{18}$$

where r is burning rate of the propellant, A_b is the burning surface area of propellant, and ρ_p is the density of propellant. The mass discharge

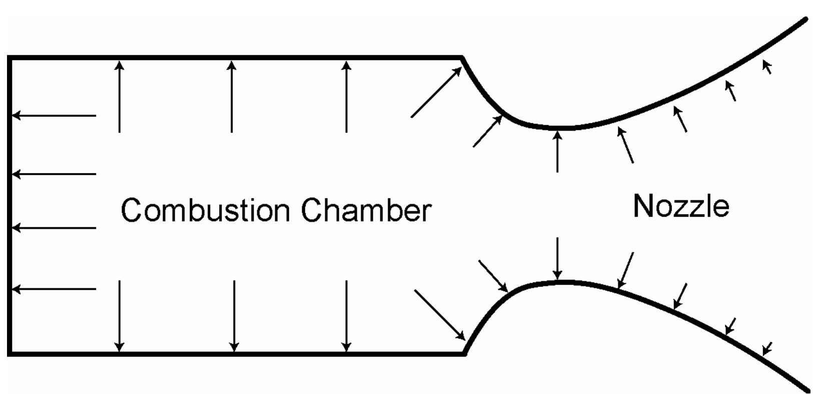

Figure 4. Pressure distribution in the combustion chamber and the nozzle of a rocket motor.

rate from the nozzle, $\dot{m}_d$, is given by

$$\dot{m}_d = c_D A_t p_c \tag{19}$$

where A_t is the cross-sectional area of the throat, p_c is the chamber pressure, and c_D is the nozzle discharge coefficient given by

$$c_D = \left(\frac{M_g}{RT_g} \frac{2}{\gamma + 1} \right)^{\frac{\gamma+1}{\gamma-1}} \tag{20}$$

Equation 20 shows that c_D is dependent on the combustion properties of propellant such as combustion temperature T_g, molecular mass M_g, and γ is the ratio of specific heats at constant pressure to the specific heat at constant volume for the combustion product. The universal gas constant R is defined by $R = R_g M_g$, where R_g is the gas constant of the combustion product.

The mass balance of the rocket motor at steady state is given by

$$\dot{m}_g = \dot{m}_d \tag{21}$$

Using equations 18, 19 and 21, the chamber pressure is determined to be

$$p_c = \frac{\rho_p K_n r}{c_D} \tag{22}$$

where $K_n = A_b / A_t$, which is determined by the physical dimension of the rocket motor design. In general, the burn rate of propellant increases linearly as pressure increases in a ln p versus ln r plot at constant initial temperature T_0, where r is burn rate and p is pressure. Thus, the burn rate is represented by the experimental law, Vieille's law or Saint Robert's law as

$$r = ap^n \tag{23}$$

where n is the pressure exponent of burn rate and a is a constant based on the initial propellant temperature T_0. Substituting equation 23 into equation 22, one gets

$$p_c = \left(\frac{a \rho_p K_n}{c_D} \right)^{\frac{1}{1-n}} \tag{24}$$

The mass balance of a rocket motor is illustrated in Figure 5. The chamber pressure p_c is at the intersection of the straight line $\dot{m}_d$ and the curved line of $\dot{m}_g$. It is evident that the intersection point is a stable point only when the pressure exponent n is less than unity. When $n > 1$, $\dot{m}_g$ becomes larger than $\dot{m}_d$ and the chamber pressure increases slightly. As a result, the rate of gas generation becomes greater than the rate of mass discharge, and the chamber pressure increases to an even higher pressure—usually resulting in an explosion. On the other hand, if the chamber pressure should decrease slightly, $\dot{m}_d$ becomes larger than $\dot{m}_g$. As a result, the chamber pressure decreases to atmospheric pressure.

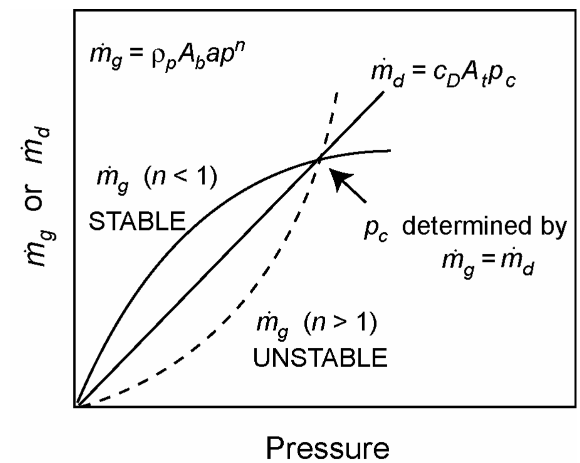

Figure 5. Mass balance of the mass generation in the chamber and the mass discharge from the nozzle showing the conditions of stable and unstable burning.

3.3 Thrust and Specific Impulse

Once the thrust required is determined, the mass generation rate $(\dot{m}_g)$ of the propellant grain in the rocket motor is determined by the following relationship:

$$F = \dot{m}_g I_{sp} \tag{25}$$

where I_{sp}, the specific impulse, is determined by[1–4]

$$I_{sp} = \frac{1}{g}\sqrt{\frac{2\gamma}{\gamma-1}\frac{RT_g}{M_g}\left\{1-\left(\frac{p_e}{p_c}\right)^{\frac{\gamma-1}{\gamma}}\right\}} + \frac{1}{g}\left(\frac{\gamma+1}{2}\right)^{\frac{\gamma+1}{2(\gamma-1)}}\sqrt{\frac{RT_g}{\gamma M_g}}\left(\frac{p_e-p_a}{p_c}\right)\frac{A_e}{A_t} \quad (26)$$

where T_g is the combustion temperature, M_g is the molecular mass of the combustion products, γ is the specific heat ratio, R is the universal gas constant, A_e is the cross-sectional area of the nozzle exit, p_e is the pressure at the nozzle exit, p_a is atmospheric pressure, and g is the gravitational acceleration. This shows that I_{sp} is a function of not only the energetics of the propellant but also the expansion ratio of the nozzle, which is determined by ratio of the nozzle exit area to the throat area and the ambient atmospheric pressure. The maximum specific impulse ($I_{sp,max}$) is obtained when the nozzle exit pressure is equal to atmospheric pressure (i.e., $p_e = p_a$) as

$$I_{sp,max} = \frac{1}{g}\sqrt{\frac{2\gamma}{\gamma-1}\frac{RT_g}{M_g}\left\{1-\left(\frac{p_e}{p_c}\right)^{\frac{\gamma-1}{\gamma}}\right\}} \quad (27)$$

This condition is obtained when the expansion ratio is chosen to be an optimum expansion ratio as described in Reference 2.

The thrust of a rocket motor is expressed by[1–3]

$$F = c_F A_t p_c \quad (28)$$

where F is thrust, p_c is pressure in the combustion chamber, and c_F is the so-called "thrust coefficient", which is determined by the nozzle expansion ratio of the rocket motor as given by

$$c_F = \sqrt{\frac{2\gamma^2}{\gamma-1}\left(\frac{2}{\gamma-1}\right)^{\frac{\gamma+1}{\gamma-1}}\left\{1-\left(\frac{p_e}{p_c}\right)^{\frac{\gamma-1}{\gamma}}\right\}} + \left(\frac{p_e-p_a}{p_c}\right)\frac{A_e}{A_t} \quad (29)$$

This shows that c_F is only dependent on the expansion ratio of the divergent part of the nozzle and is independent of the combustion performance of the propellant in the combustion chamber. The maximum thrust coefficient ($c_{F,max}$) is obtained when the pressure at the nozzle exit (p_e) is equal to the atmospheric pressure (p_a). Thus, $c_{F,max}$ is given by

$$c_{F,max} = \sqrt{\frac{2\gamma^2}{\gamma-1}\left(\frac{2}{\gamma-1}\right)^{\frac{\gamma+1}{\gamma-1}}\left\{1-\left(\frac{p_e}{p_c}\right)^{\frac{\gamma-1}{\gamma}}\right\}} \quad (30)$$

In general, c_F is approximately 1.4–1.5 for low altitude operation and 1.5–1.6 for high altitude operation when the nozzle is designed to gain an optimized expansion ratio. The overall performance of a rocket motor is given by I_{sp}, which consists of two parameters:[1–3] the performance of combustion in the rocket motor represented by T_g / M_g and the performance of the nozzle represented by c_F.

3.4 Pressure Sensitivity of Burn Rate

The pressure sensitivity of burn rate is expressed as[1–5]

$$n = \frac{\mathrm{d}\ln r}{\mathrm{d}\ln p} \quad \text{at constant } T_0 \quad (31)$$

The burn rate also increases as T_0 increases at constant pressure. A typical example of the results obtained by a strand burner at $T_0 = 233$ and 333 K is shown in Figure 6. The temperature sensitivity of burn rate, σ_p, is defined as the fraction of burn rate increase when the initial propellant temperature of 273 K is increased at constant pressure as

$$\sigma_p = \frac{\dfrac{r_1 - r_0}{r}}{T_1 - T_0} \quad (32)$$

where r_0 and r_1 are the burn rates at temperatures T_0 and T_1, respectively. The differential form of σ_p is

$$\sigma_p = \frac{\mathrm{d}\ln r}{\mathrm{d}T_0} \quad \text{at constant } p \quad (33)$$

Substituting equation 23 into equation 33, one gets

$$\sigma_p = \frac{\mathrm{d}\ \ln\left(ap^n\right)}{\mathrm{d}T_0}$$

at constant p, and then

$$\sigma_p = \frac{\frac{\mathrm{d}a}{\mathrm{d}T_0}}{a} \quad \text{at constant } p \tag{34}$$

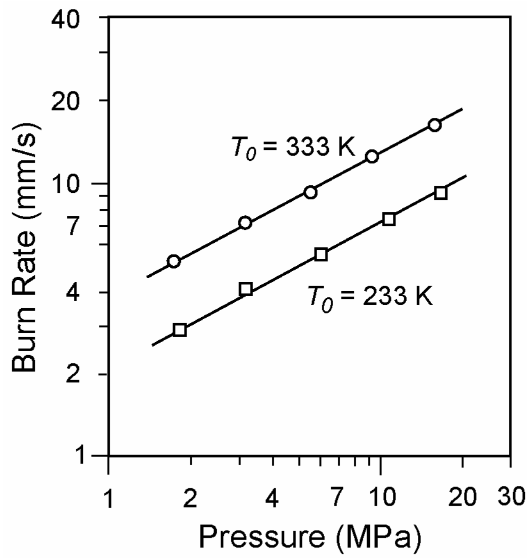

Figure 6. Burn rate versus pressure at different initial propellant temperatures.

3.5 Pressure Sensitivity of Rocket Motor

When T_0 of the propellant in the combustion chamber is changed, p_c is changed according to the relationship of equation 24. The pressure sensitivity of a rocket motor, π_k, is defined as[1–5]

$$\pi_k = \frac{\frac{p_{c_1} - p_{c_0}}{p_c}}{T_1 - T_0} \quad \text{at constant } K_n \tag{35}$$

where p_{c_1} and p_{c_0} are the chamber pressures at T_1 and T_0, respectively. The differential form of equation 35 is given by

$$\pi_k = \frac{\mathrm{d}\ln p_c}{\mathrm{d}T_0} \quad \text{at constant } K_n \tag{36}$$

Substituting equation 24 into equation 36, one gets

$$\pi_k = \frac{\frac{\mathrm{d}a}{\mathrm{d}T_0}}{a(1-n)} = \frac{\sigma_p}{1-n} \tag{37}$$

Thus, it should be noted that the temperature sensitivity of burn rate σ_p and the pressure exponent of burning rate n are the two important parameters to determine the chamber pressure p_c (i.e., the thrust of the rocket motor as shown by equation 28 at different initial propellant temperatures).

Figure 7 shows a typical result of rocket motor firing tests at $T_0 = 233$ and 333 K (constant K_n). The propellant used is hydroxyl-terminated polybutadiene (HTPB) / ammonium perchlorate (AP) composite propellant composed of $\xi(\mathrm{AP}) = 0.84$ with $\sigma_p = 0.003$/K and $n = 0.5$ ($\pi_k = 0.006$/K). It is important to note that the chamber pressure increased from 4.9 MPa ($T_0 = 233$ K) to 8.0 MPa ($T_0 = 333$ K).

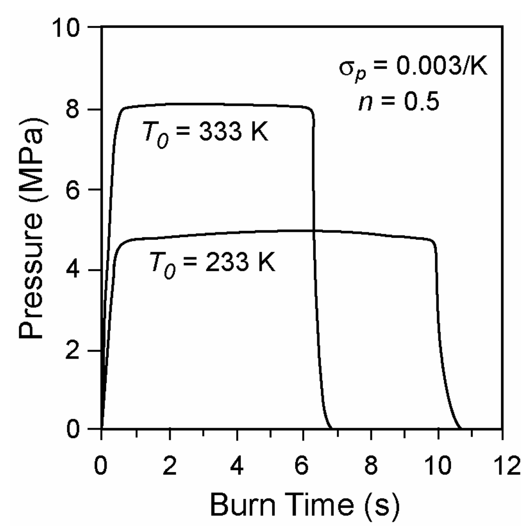

Figure 7. Firing test results of a rocket motor at different temperatures.

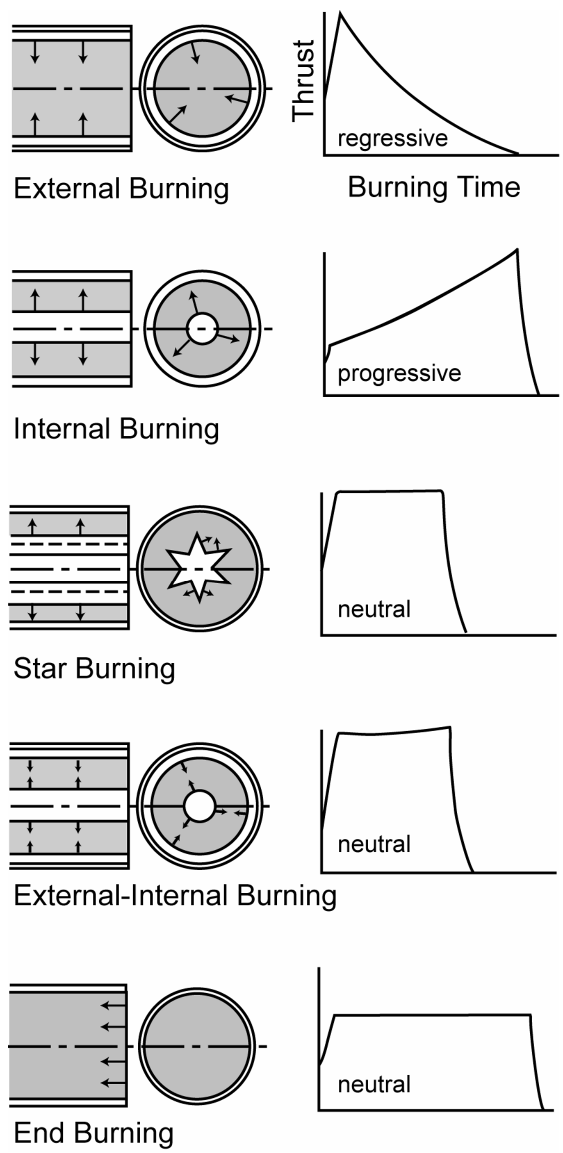

Figure 8. Propellant grains and their thrust (pressure) versus burning time.

4. Propellant Grain Design

4.1 Thrust Versus Burning Time

The thrust generated by the burning of a propellant grain is determined by the mass burn rate and the mass discharge from the nozzle. The mass burn rate is dependent on the linear burn rate, burning surface area, and propellant density. The burning time t_b is given by

$$t_b = \frac{L_b}{r} \tag{38}$$

where L_b is the length or thickness of the propellant grain and is termed "web thickness". The burning surface area A_b is dependent on the grain geometry.

Figure 8 shows typical propellant grain shapes to gain various types of thrust versus burning time relationships.[1] The external burning—from the outside of a cylindrical grain—generates a regressive thrust as the burn time increases. On the other hand, an internal burning grain from the internal surface of a hole in a cylindrical grain generates a progressive thrust as burning time increases. A star-shaped internal burning generates a neutral burning (i.e., the area remains relatively unchanged during burning). The external-internal burning cylindrical grain generates a neutral burning. An end burning cylindrical grain also generates a neutral burning.

Figure 9 shows various types of granulated propellant grains used for guns and pyrotechnics. Since a large number of the granulated grains burn simultaneously in a combustion chamber, the burning surface area A_b is significantly higher than the propellant grains shown in Figure 8; also the mass burning rate of the granulated grains is high. The chamber pressure becomes high due to high K_n based on equation 22, and the thrust becomes high. On the other hand, the burning time t_b becomes very short, based on equation 38, since the web thickness of the granulated grains is very thin.

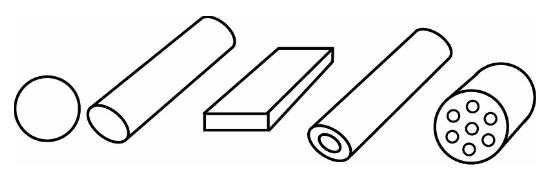

Figure 9. Various types of granulated propellant grains.

Internal burning grains are commonly used for solid rocket motors to protect the chamber wall from the high temperature gas generated by the propellant combustion. The side chamber wall is exposed only when the burning of the grain is complete. Thus, the heat insulation of the chamber wall is not a major issue for the motor design. Figure 10 shows typical cross

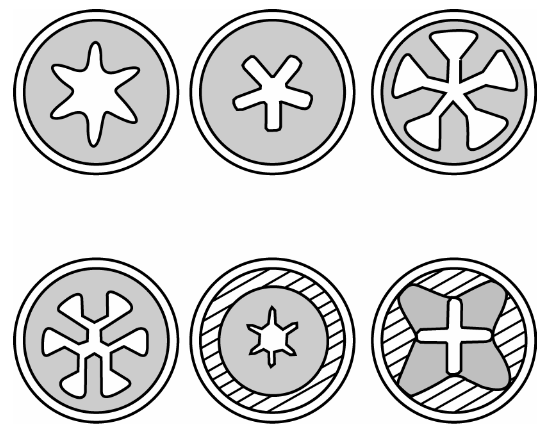

Figure 10. Cross-sections of perforated internal-burning propellant grains.

sections of perforated propellant grains, such as star-shaped, wagon-wheel-shaped, and dendrite-shaped. Two or more different propellant layered grains are also used to gain various types of thrust versus burning time.[1]

Since rocket projectiles are generally launched from the ground or from low speed carriers, and the initial speed of the projectile is low, a high thrust is required to gain stabilized flight of the initial stage to protect the rocket motor from side wind effects and/or to avoid tip-off from launchers. Thus, the thrust of a rocket motor often consists of two phases, booster phase and sustainer phase. When the thrust ratio of the booster and sustainer phases is not high, the required thrust versus burning time curve is attained. However, when the ratio is high, two propellant grains are needed: a high burn-rate grain for the booster phase and a low burn-rate grain for the sustainer phase. Figure 11 shows typical combinations of two grains and internal and/or end burning type of grains to obtain high thrust ratios of booster and sustainer phases.

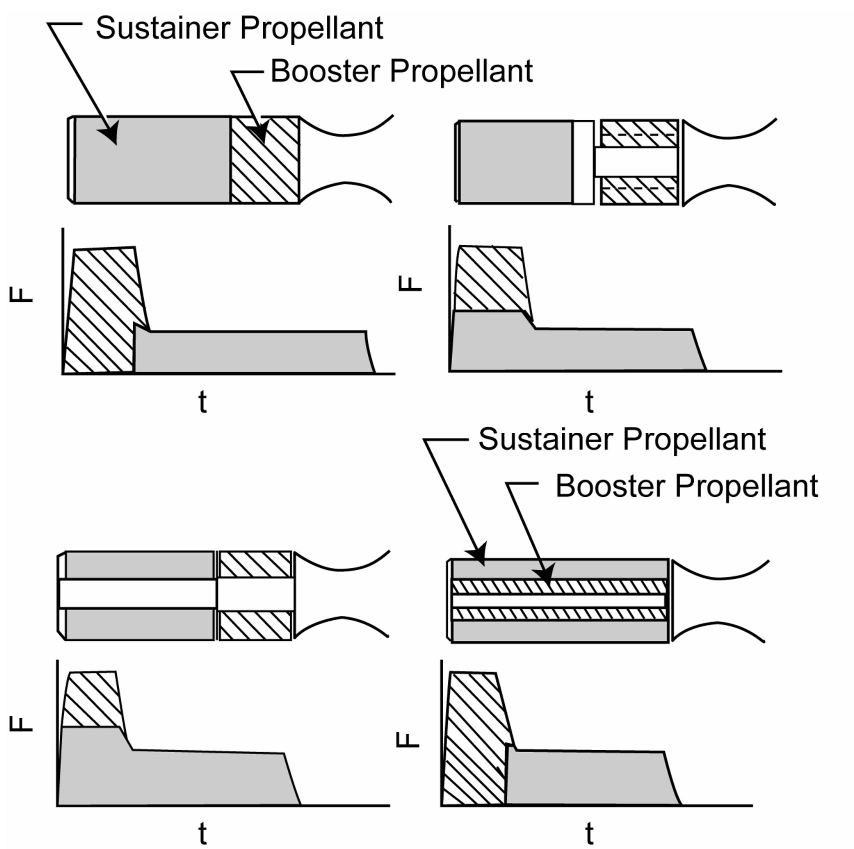

Figure 11. Some typical combinations of two propellant grains in a rocket motor.

4.2 Grain Design Concept

The selection of propellant for a specific requirement for a practical rocket motor design is based on the specific impulse, combustion temperature, exhaust products and the relationship of burn rate and pressure. This includes the value of the pressure exponent and temperature sensitivity of burn rate. The burn rate is increased by the cross-flow in the port of the internal burning grain, the so-called erosive burning. In the case of aluminized propellants, the local burning rate of the burning surface of an internal burning grain is increased under a centrifugal acceleration. Furthermore, an oscillatory burning occurs in a rocket chamber when the burn rate response of the propellant is matched to the acoustic mode of the free volume of the chamber. These combustion phenomena must be examined prior to the practical grain design.[6–10]

Once a propellant is chosen, the following three parameters are taken into account for the propellant grain design:

1) Burning area versus burning distance (also referred to as "web thickness")
2) Mechanical stress analysis
3) Anti-aging analysis

The thrust versus burning time requirement is obtained by the selection of the propellant grain combinations or the perforation of the grain shape.[6–8] Since the propellant grain in a rocket chamber encounters various mechanical stresses from the high axial and/or radial acceleration or by the temperature change of the grain, a mechanical stress analysis is required. If the rocket motor is used even after a decade, an anti-aging analysis is required to maintain its design performance.

4.3 Selection of Propellants

A propellant composed of ammonium perchlorate (AP) as the oxidizer and hydrocarbon polymer as the fuel component is the so-called "AP composite propellant" and is commonly used. Hydroxyl-terminated polybutadiene (HTPB) or carboxyl-terminated polybutadiene (CTPB) is used as a fuel component and as a binder to adhere to the AP particles to form a propellant grain. AP composite propellants are widely used for space launch rockets and missile rockets because of their wide range of burning rate characteristics, relatively safe production, low sensitivities to friction and mechanical shock, and low production cost. The mechanical properties such as stress strength, elongation, and elasticity are chosen based on the required ballistic characteristics. The burning rate characteristics expressed by equation 23 are managed by the choice of AP particle sizes, solids loading and burn rate catalysts. When a high burning rate is needed, small AP particles are used. Furthermore, the burning rate is increased by the addition of a small amount of iron oxide (e.g., 1% Fe_2O_3) and is decreased by the addition of lithium fluoride (e.g., 1% LiF).

The specific impulse defined in equation 26 is increased by the addition of fine aluminum powder to AP composite propellants, for example, I_{sp} is increased about 7 % by the addition of 15% Al. However, large amounts of white smoke are formed as combustion products from the formation of aluminum oxide (Al_2O_3) particles. Though the exhausted white smoke does not interfere with any application of space launch rockets, it must be eliminated from tactical rockets to avoid detection of the launch sites or ballistic trajectories. When no aluminum particles are added to AP composite propellants, no generation of solid particle white smoke occurs. This class of AP composite propellants is called "reduced smoke propellants" and is used for air-to-air missiles and surface-to-air missiles. However, when the humidity in the atmosphere is much above 70% or the temperature in the atmosphere is much below 250 K (–23 °C), white smoke is generated by the hydrogen chloride (HCl) produced by the AP particles used as the oxidizer. The hydrogen chloride exhausted from rocket nozzles into the atmosphere provides nuclei to form water mists with the high humidity of the atmosphere or reacts with water from the combustion products exhausted to a low temperature atmosphere.

If one requires smokeless exhaust gas—even under high humidity conditions—double-base propellants or ammonium nitrate (AN) based composite propellants are used. Since these propellants are composed of halogen-free ingredients, no visible smoke is formed even when the humidity in the atmosphere is high. Since double-base propellants are composed of nitrate esters such as nitroglycerin and nitrocellulose, the cost of production is relatively high and the mechanical properties are inferior to AP composite propellants. The disadvantage of using AN as an oxidizer is that the specific impulse is low and strict humidity control is needed during the production process because of the hygroscopic nature of AN.

5. Design of Rocket Motor Case and Thermal Protection

5.1 Size and Shape of Rocket Motor Case

The chamber of a rocket motor case is used as the container for a propellant grain and is also used to burn the propellant grain under conditions of high pressure and high temperature. The size of the chamber is determined by the volume of the propellant grain required to generate the total impulse. The chamber pressure in the motor is given by the required thrust and the nozzle throat area as

$$p_c = \frac{F}{c_F A_t}$$

The thickness of the chamber wall is determined by the size and the mechanical properties of the material used for the motor case. Although the combustion pressure changes during burning due to the changing burning surface area of the propellant grain, the wall thickness must be determined by the maximum chamber pressure $p_{c,max}$ during burning. In addition, a safety margin of the wall thickness must be taken into account, for example, $1.2 \times p_{c,max}$.

In general, rocket motor cases are cylindrical and slender in shape. This is because of the reduction of aerodynamic drag during flight and the cost reduction of the machining process of the case materials. The ratio of the diameter to the length is determined by the flight dynamics of the rocket projectile.

In the case of outer atmospheric flight aerodynamics, drag is not considered. Spherical shaped motor cases are used for the upper stage of space rockets to gain advantage of the minimized wall thickness at a given combustion pressure. However, the cost of production is much higher compared to that of cylindrical motor cases.

5.2 Materials Used for Motor Cases

Many types of materials are used for the rocket motor cases.[3,7,8] Modern rocket motors are made of carbon composite materials having mechanical properties that are superior to those of metals. However, the cost of these materials is relatively high unless there is mass production as for small motors and very large motors such as space rocket boosters and ICBM rocket motors. Medium-sized motors such as air-to-air missiles and anti-tank missiles are made of steel or titanium alloy because of the favorable ratio of mechanical strength to density. This is evident from the mechanical strength and elongation characteristics of the materials.

For commercial use of rocket motors such as the launch of hobby rockets, launch of fireworks, life-saving signal rockets, and lightning-earth rockets, the motor cases are made of paper or plastic. The advantages of these materials are greater safety when the empty motor case falls to the ground after burnout and low production cost. However, a high safety margin for wall strength must be taken into account to avoid any unexpected manufacturing or material irregularities from the motor cases.

5.3 Thermal Protection

Since the combustion temperature in rocket motors is typically greater than 2000 K, the chamber wall should be protected from heat. The temperature of the interior of the propellant grain remains at the initial temperature of the grain in an operating motor until the burning surface approaches. Thus, the chamber wall is isolated from the combustion zone temperatures as long as the wall is covered by the propellant grain.

However, when a part of the propellant grain is burned completely, the interior wall surface is exposed to the high temperature combustion gas. Then, the wall is thermally eroded and can be burst by the combustion pressure. To protect the casing from the combustion gas, a heat insulating material is added to the interior surface of the chamber wall. The heat insulting material typically consists of rubber sheets that are adhered to the chamber wall. The propellant is then cast into the chamber (direct cast method) or the propellant grain is inserted into the chamber (freestanding method). An important parameter for the direct case method is to assure the complete adhesion between the insulation and the propellant after curing of the propellant.

The thickness of the insulation depends on the duration of exposure to the combustion gas and on the location within the chamber. When the propellant grain is of an end-burning geometry, the aft (nozzle) end of the insulation is exposed from ignition to burnout. Thus, a thicker sheet of insulation is needed at the nozzle (aft) end.

6. Design of Nozzle

6.1 Size and Shape of Nozzle

Rocket nozzles are used to convert the low-velocity combustion gases in the chamber to high velocity exhaust through thermodynamic processes. In other words, conversion is through expansion. Once the chamber pressure p_c and the nozzle throat area A_t are determined, the expansion ratio ε defined by the area ratio of the nozzle exit area A_e and A_t is determined thermodynamically. The thrust coefficient c_F, defined by equation 29, indicates the efficiency of the nozzle. The maximum thrust coefficient $c_{F,max}$ is determined by the chamber pressure p_c and the atmospheric pressure p_a. The optimum expansion ratio ε_{max} increases because p_a decreases with altitude. Chamber pressure p_c is unaffected by anything past the throat of the rocket motor.

During the process of nozzle design the nozzle throat area (A_t) is determined first based on the thrust requirement, and then the nozzle exit area (A_e) is determined to gain an optimum expansion ratio. It is evident that the shorter the length of the nozzle, the lower the nozzle mass. The convergent nozzle angle is larger than the divergent nozzle angle because of the subsonic flow and the decreasing pressure along the nozzle wall towards the throat of the nozzle. Thus, no flow separation in the boundary layer occurs from the convergent nozzle wall.

On the other hand, the divergent nozzle angle is important to gain a smooth pressure gradient and to minimize the friction loss caused by the nozzle wall and the supersonic exhaust gas flow. In general, the expansion angle is limited to approximately 30° to gain smoothly expanded gas flow, to minimize the friction loss of the supersonic flow, and to limit vector losses in the nozzle. The convergent and divergent parts of the nozzle are connected at the nozzle throat. (See Figure 3.)

When the pressure at the nozzle exit (p_e) is higher than the local atmospheric pressure (p_a), the nozzle is considered to be under-expanded, and when p_e is smaller than p_a, the nozzle is considered to be over-expanded. The specific impulse (I_{sp}) is less for both cases when compared to the optimum expansion ratio as shown in equation 26. When the trajectory of a rocket projectile varies from a low altitude to a high altitude, the atmospheric pressure decreases as the altitude increases. As a result, the nozzle expansion ratio must be altered to gain an optimum expansion ratio as long as the combustion pressure remains constant. Since the geometry of a conventional nozzle is fixed, the optimum expansion is set for a specific altitude and chamber pressure.

6.2 Materials Used for Nozzle

Since rocket nozzles are exposed to high temperature and high velocity combustion gas during propellant burning, the heat flux from the gas to the nozzle wall is significantly higher than in the combustion chamber. The maximum heat flux is at the nozzle throat (approximately 2 MW/m^2 for conventional AP composite propellants). In addition, the mechanical stress acting on the interior surface of the nozzle is approximately 10 MPa for a typical ground launched rocket motor.

As shown in equation 28, the nozzle throat (A_t) is an important parameter to attain an expected performance of thrust versus time for operation. A change of A_t (throat erosion) changes p_c and then c_F, which changes F significantly. To avoid the change in A_t, high temperature resistant materials are used not only for the nozzle throat but also in the convergent and divergent parts of the nozzle. Typical and conventional materials used for nozzles are graphite (carbon) because the combustion products of solid propellants are generally fuel rich gases and graphite (carbon) are not oxidized by the gas flow. High-density graphite is commonly used for modern rocket motors to resist not only these high temperatures but also erosion by sonic or supersonic flow. The density of a graphite nozzle for practical applications is approximately 1.9×10^3 kg/m^3. The high-density graphite also protects the casing from mechanical damage from the thermal shock during the ignition stage. When the heat flux is much higher, the nozzle surface is damaged and A_t increases. Also, ceramics such as aluminum oxide or zirconium oxide can be coated on the interior surface of the nozzle by a plasma torch. [Note: Aluminized propellants form an aluminum oxide coating on the throat, especially at and just after ignition, which reduces A_t.]

When the size of a motor case is small (less than about 50 mm in diameter), the size of the nozzle is also small. In this instance, the convergent and divergent parts of the nozzle, including the throat, are usually made of graphite. The mechanical stress acting on the interior surface of the nozzle is not high because the interior diameter is small. However, the mechanical stress increases as the diameter of the throat increases, and graphite becomes insufficient to protect the nozzle from damage. In general, a larger nozzle is separated into three parts (i.e., convergent, throat, and divergent). Since the heat flux and the flow velocity at the convergent and divergent parts are relatively small when compared to the throat, glass fiber reinforced plastics (GFRP) with phenolic or epoxy resin are commonly used for the other parts. An ablative process due to the melting and gasification of the glass fibers and plastic resins of GFRP effectively act to protect the nozzle from high heat flux.

Carbon fiber reinforced plastics (CFRP) with various types of plastic resins are also used for the convergent and divergent parts. Though no ablative effect is expected for the carbon fibers of CFRP, the superior heat resistant properties of the carbon fibers protect the parts from heat and gas flow. In addition, the mechanical properties of CFRP, such as stress strength and density, are superior to those of GFRP. When reduction of the nozzle mass is an important parameter to obtain high performance of rockets such as a third of a four-stage motor used at high altitude, carbon-carbon (C/C) is used for the nozzle system including convergent, throat, and divergent parts. Though C/C is the best material for rocket nozzles, at present time, the cost of C/C is extremely high and the application is highly limited.

7. Design of Igniter

7.1 Ignition Transient

An igniter is used to ignite the surface of the propellant grain set in a combustion chamber. When an igniter is operated, hot gas and/or particles are applied to the surface of the propellant grain in the combustion chamber. The ignited surface generates high temperature combustion gases and the chamber pressure increases. The ignited surface area increases along the grain surface. During this ignition process, the burn rate is not given by equation 23, which is only effective for steady state burning.

The ignition process of the propellant grain includes the temperature rise of the grain surface, heat conduction into the grain, gasification at the surface, and production of sufficient gases to raise the chamber pressure. When the igniter charge, the so-called "pyrolant" (pyrogen) —which is an energetic material—burns, this causes a spike in the pressure. This results in a rapid onset and decay that can "shock" the system, possibly causing failures. In addition, the heat flux generated by the pyrolant must be enough to ignite the grain surface, enabling the pressure of steady-state combustion to be reached within a required short duration.

The ignition transient depends on the type of pyrolants and propellants. Two types of pyrolants are used for igniters: high-volume gas producing and high temperature particle producing. Black Powder produces more gaseous products than pyrolants composed of metallic particles and crystalline oxides. Since the chamber pressure of a double-base propellant rocket motor requires more than 4 MPa to reach steady-state combustion, Black Powder is often used as a pyrolant for this class of rocket motors.

On the other hand, composite propellants, such as ammonium perchlorate or ammonium nitrate-based composite propellants, require high heat flux to raise the burning surface temperature and to gasify the grain surface. High temperature hot spots are made on the grain surface when metal particles are used as a component of pyrolants. The metal particles are oxidized by the other components, crystalline oxidizers, generating high temperature hot spots dispersed on the grain surface. The grain surface at each hot spot is ignited by the heat conduction from the hot spot and the burning area spreads along the entire grain surface.

The heat flux that must be applied to a propellant grain surface for ignition is dependent on the chemical ingredients, the physical shape of the grain and the type of igniter ingredients. In general, high pressure is needed for the ignition of double-base propellant grains in a rocket motor. The minimum pressure is approximately 4 MPa to reach a steady state burning to satisfy the mass balance relationship given by equation 21 since the combustion temperature of double-base propellants decreases rapidly below 4 MPa. The mass discharge rate $\dot{m}_d$ given by equation 19 increases more than expected if one assumes c_D given by equation 20 is constant. The mass discharge coefficient c_D increases as pressure decreases.

Since AP composite propellants burn stably even below 0.1 MPa and the temperature of the combustion products is relatively independent of pressure, c_D remains constant throughout ignition pressure to the steady-state pressure. When even a part of the grain surface is ignited, the burning surface increases due to the flame spreading phenomena along the grain surface, and the chamber pressure increases until the pressure reaches the steady-state pressure given by equation 24.

Since AN particles mixed within an AN composite propellant decompose endothermically, a high heat flux is needed to gasify the AN particles. Furthermore, the AN particles melt and form a molten layer on the burning surface of the propellant and absorb much energy to generate combustible gas for ignition. Accordingly, the ignitability of AN composite propellants appears to be inferior to that of AP composite propellants.

7.2 Pyrolants Used for Igniters

The typical materials used for the pyrolants of igniters are the physically mixed particles of boron and potassium nitrate (B-KN), zirconium and ammonium perchlorate (Zr-AP), and magnesium and polytetrafluoroethylene (Mg-TF). The particles of boron (B), zirconium (Zr), or magnesium (Mg) are oxidized to produce their oxides, and they generate high temperature particles. These particles are showered onto the igniting surface of the propellant grains.

Although boron particles are not metal particles, they act like metal particles similar to aluminum, zirconium, or magnesium. When boron particles are oxidized by the gaseous nitrogen oxides produced by the thermal decomposition of crystalline potassium nitrate (KNO_3) particles, high temperature (greater than 4000 K) boron oxides are formed. Similar to boron particles, zirconium particles are oxidized by the gaseous perchloric acid produced by the thermal decomposition of crystalline ammonium perchlorate (NH_4ClO_4) particles.

Polytetrafluoroethylene (TF) is a polymeric material that produces fluorine gas when it thermally decomposes. The fluorine gas oxidizes the magnesium particles to produce magnesium fluoride (MgF_2) particles that are agglomerated during the process of the oxidation reaction. High-temperature (greater than 3500 K) particles are showered onto the propellant grain surface. The hot particles of boron oxide, zirconium oxide, or magnesium fluoride act as hot spots to transfer heat to the grain surface and gasify the propellant ingredients. Once thermal gasification occurs on the propellant grain surface, an exothermic reaction proceeds to ignite the gases and the pressure in the rocket chamber rises.

The pyrolants are ignited indirectly by very thin wires that are electrically heated. These wires are made of platinum or other electrically resistive metals of about 30 μm in diameter. When an electric current is applied to the wires, heat is generated due to the electric resistance of about 400 Ω/m. Generally, the platinum wires are coated with mixtures of nitrocellulose, potassium perchlorate ($KClO_4$), and fine metallic particles. This mixture is first ignited, and then the heat produced by the combustion of the mixture ignites the pyrolants successively.

The pyrolant and hot wires are set an igniter case that is made of a metal or plastic material. A number of holes are made on the side of the case wall to shower the burning hot gas and particles on the surface of the propellant grain. For large rocket motors, such as the space shuttle booster or an ICBM rocket motor, ignition is accomplished by using a small rocket motor that is attached at the top end of the inside of the motor. Once the small motor is ignited, the exhaust gas from the nozzle ignites the large interior surface of the propellant grain.

8. Combustion Phenomena in a Rocket Motor

Combustion in a rocket motor includes various phenomena such as ignition transient, flame spread, erosive burning, oscillatory burning, unstable burning, and burning interruption.[1,8] These phenomena are highly dependent on the physicochemical properties of propellant grains.

8.1 Erosive Burning

Erosive burning occurs at an early stage in the burning of a propellant grain when the cross-sectional area of the gas flow channel inside the grain, the so-called “port area”, has a value close to that of the nozzle throat area. When the port area is equal to the nozzle throat area, the flow velocity at the aft end of the grain reaches sonic velocity (i.e., 300 m/s at normal temperatures, which varies with flame temperature, pressure and composition). Since the heat flux transferred back from the gas flow to the burning grain-surface increases when the cross-flow velocity is high, the burn rate of the grain increases compared with that of no gas flow. The burn rate expressed by equation 23 is no longer valid. As the port area increases, the cross-flow velocity decreases and the erosive burning effect diminishes.[1,2]

When erosive burning occurs, the pressure in the combustion chamber increases. The increased pressure increases the burn rate given by equation 23. It is important to take account of the increased pressure of erosive burning to obtain a required thrust versus burning time relationship.

8.2 Stable and Unstable Combustion

Oscillatory burning occurs in the chamber when a standing wave is established between the facing grain surfaces or between the fore-end and aft-end of the chamber. The standing pressure wave in the chamber enhances the burn rate of the propellant grain. The oscillatory frequency is dependent on the size of the internal port of the grain or the length of the motor. No oscillatory burning is observed when an end-burning type grain is used. When the oscillatory mode is in resonance with the burn-rate mode of the propellant grain, the overall mass-burn-rate is increased, and then the pressure in the chamber is increased drastically.[1,2]

Figure 12 shows the cross-section of an extinguished propellant grain obtained from a nozzle separation.[1,2] The nozzle separation was caused by the increased pressure that was the result of an irregular burning. The grain was a six-pointed star shaped composition of AP/HTPB propellant. Immediately after the grain was ignited, at 0 seconds, the chamber pressure increased as expected as shown in the measured DC pressure curve. However, a strong peak of AC pressure was generated at t_b seconds after ignition. The extinguishing of the propellant occurred due to the rapid pressure decay. The cross-section of the grain after being extinguished at time t_b seconds was the same shape as expected at the steady state burning. The results indicate that the resonant burning occurs with a specific grain shape.

When a small quantity of solid particles such as aluminum or zirconium was added to the propellant grain, no pressure peaks were generated and a steady state burning was conducted until the propellant grain was completely consumed. The solid particles absorb the energy of oscillation and damp the observed oscillatory combustion when the generated oscillation is in the range of acoustic mode, approximately 500 Hz.

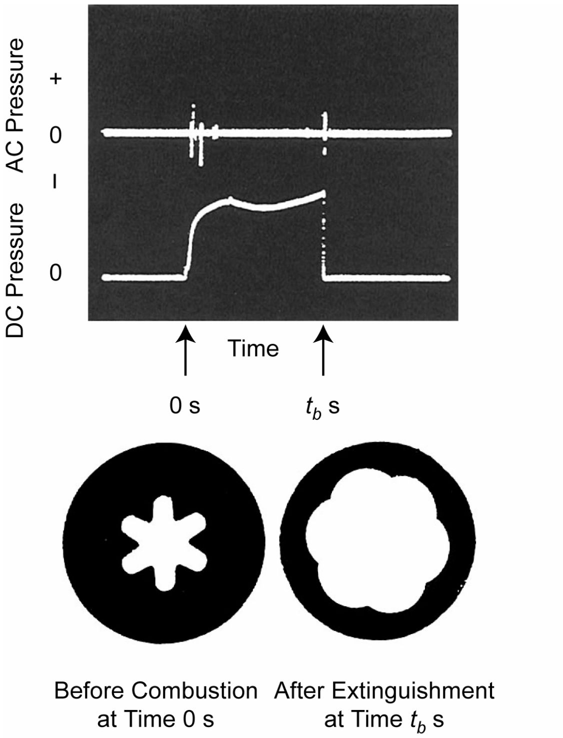

Figure 12. DC and AC pressures in a rocket combustion chamber and cross-sections of the propellant grain before combustion and after being extinguished.

When a high-pressure oscillation is induced along the radial axis of the chamber, a rod can be set in the center axis of the port of the grain to alter the resonance acoustic mode of the radially directed oscillation. The rod is made of a ceramic-coated metal to resist the high temperature combustion gas in the chamber.

When a low-frequency oscillation is induced along the axis of the chamber, physical separation of propellant grain by some insulation acts effectively to change the oscillatory mode.

When a non-acoustic mode of oscillation occurs, no oscillatory damping effect is accomplished by the addition of metal particles because the size of the particles is much smaller than the traveling oscillatory wavelength. However, the burning grain acts as a damping material if the shape of the grain is chosen to absorb the traveling pressure wave adequately.

8.3 Combustion under Centrifugal Acceleration

A spinning motion along the axis of a rocket projectile is provided to stabilize the vehicle and improve the flight trajectory. The spinning motion is created aerodynamically either by the fins attached to the projectile or by the nozzle fins attached to the interior surface of the nozzle, similar to thrust vector control fins. The centrifugal acceleration caused by the spinning motion affects the burn rate of the propellant grain, and then the thrust versus burning time is varied as compared to the case of no centrifugal acceleration.[9,10]

The combustion gas in the port of an internal burning grain flows along the burning surface towards the nozzle when no centrifugal acceleration is given. When a centrifugal acceleration is given, a pressure gradient towards the radial direction in the port is created and then the burn rate is increased by the increased pressure at the port surface of the grain. However, the effect of the centrifugal acceleration is trivial when the combustion products are only gaseous species.

When aluminum particles are added to a propellant grain, molten aluminum agglomerates are formed on the burning surface under the centrifugal force.[9,10] This agglomeration process occurs due to the density of the molten metal particles being higher than that of gaseous products. The size of the molten agglomerates increases as the burning of the propellant grain proceeds. Since the temperature of the molten agglomerates is high, the heat flux transferred from the agglomerates to the burning propellant surface increases. Accordingly, the local burn rate of the propellant increases and then a number of pits are formed on the burning surface.

Combustion tests of an AP/CTPB composite propellant-grain were conducted using a spinning rocket motor.[9] The propellant consisted of 76.8% AP, 15.0% CTPB and 8.2% aluminum particles. The aluminum particles were 48 μm in diameter. The burning tests were conducted at 4 MPa under the centrifugal acceleration of 60 g. Burning interruption tests were done by nozzle separation during burning. When a tubular shaped grain was extinguished, pits were formed non-uniformly on the whole surface. However, when a 6-pointed star-shaped grain was burned, pits were formed along the six points of the star as shown Figure 13. In addition, the burning surface area increased due to the formation of the pits. As a result, the pressure in the rocket motor was further increased corresponding to the relationship given by equation 24.

9. Design of Two-Stage Motors with Two Propellant Grains in One Chamber

9.1 Mass Balance of Booster Phase

To attain a high thrust ratio of the booster and sustainer stages, two different propellant grains are combined in a single combustion chamber and burned simultaneously. Figure 14 shows a typical thrust or pressure versus burn time of a two-stage motor with two propellant grains (Propellant D and Propellant C) that burn in a single chamber. Propellants D and C burn simultaneously to create the booster phase with Propellant D being completely consumed in the booster phase. Then Propellant C, which remains after the booster phase, burns continuously to create the sustainer phase.

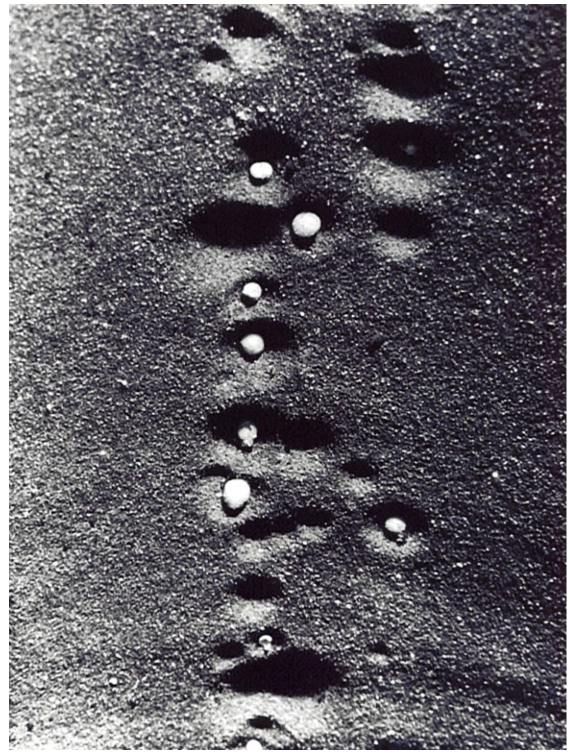

Figure 13. An extinguished burning surface of a six-pointed star-shaped aluminized AP/CTPB propellant grain.[9] Many pits are formed along each point of the star.

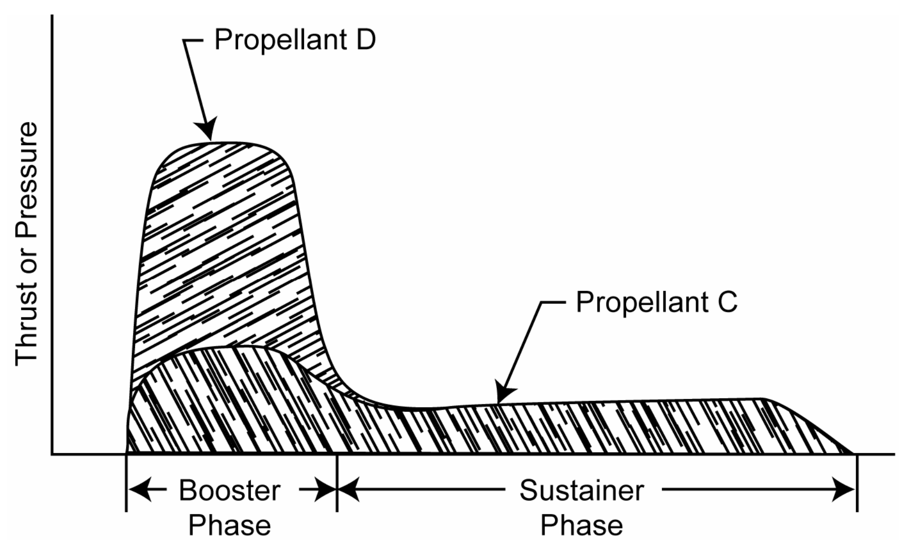

Figure 14. A two stage motor with two propellant grains in a single motor to create booster and sustainer phases.

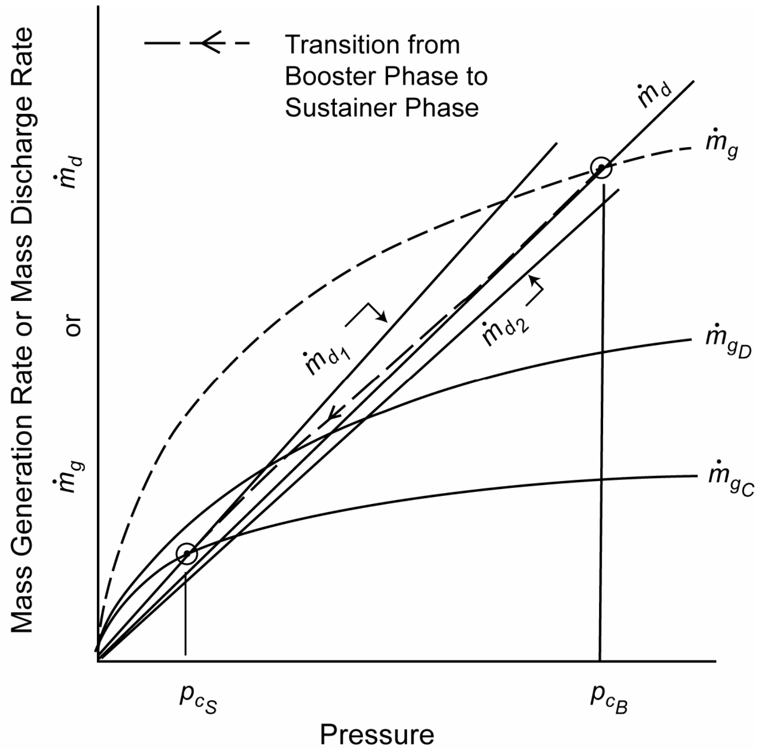

Figure 15. Mass balance in a rocket motor in which two propellant grains burn simultaneously to create the booster phase and one of propellant grain continues to burns to create the sustainer phase.

Figure 15 shows the mass balance in a rocket motor in which two propellant grains burn simultaneously during the booster phase and the one-grain that continues burning during the sustainer phase. If one assumes that the linear burning rates of Propellants D and C are given by

$$r_D = a_D p^{n_D} \quad \text{for Propellant D} \tag{39}$$

$$r_C = a_C p^{n_C} \quad \text{for Propellant C} \tag{40}$$

then the mass generation rates ($\dot{m}_{g_D}$ for Propellant D and $\dot{m}_{g_C}$ for Propellant C) at pressure p are given by

$$\dot{m}_{g_D} = a_D \rho_{p_D} p^{n_D} A_{b_D} \quad \text{for Propellant D} \tag{41}$$

$$\dot{m}_{g_C} = a_C \rho_{p_C} p^{n_C} A_{b_C} \quad \text{for Propellant C} \tag{42}$$

where the subscripts D and C denote Propellants D and C, respectively. The mass discharge rate $\dot{m}_d$ during the booster phase is given by

$$\dot{m}_{d_B} = c_{D_B} A_t p \tag{43}$$

As shown in Figure 15, the mass balance at the booster phase is expressed by the use of equation 21 as

$$\dot{m}_{d_B} = \dot{m}_{g_D} + \dot{m}_{g_C} \tag{44}$$

Substituting equations 39 to 43 into equation 44, one can determine the nozzle throat area A_t as

$$A_t = \frac{1}{c_{D_B}} \left(a_D \rho_{p_D} p^{n_D - 1} A_{b_D} + a_C \rho_{p_C} p^{n_C - 1} A_{b_C} \right) \tag{45}$$

As shown in equation 20, c_{D_B} is determined by the combustion temperature T_g, molecular mass M_g, and specific heat ratio γ of the combustion product. Since two different types of propellants burn simultaneously in a single chamber, the physical properties of the combustion products are not the mass averaged values of Propellants D and C. Both combustion products react with each other to produce an equilibrium combustion product as long as the reaction time in the chamber is sufficient. These physical values can be determined theoretically by the use of NASA SP-273 computer code[13] if one can provide the mass fractions and the chemical compositions of both Propellant D and Propellant C.

9.2 Mass Balance of Sustainer Phase

After burnout of the Propellant D grain in the booster phase, the remaining Propellant C grain continues to burn to create the sustainer phase. Since the nozzle throat area is the same as in the booster phase, A_t, determined by equation 45, the ratio of $A_b/A_t = K_n$ decreases rapidly and the pressure in the chamber decreases. As shown in Figure 15, the mass generation rate of Propellant C at the sustainer phase is given by

$$\dot{m}_{g_C} = a_C \rho_{p_C} p^{n_C} A_{b_C} \quad \text{for Propellant C} \tag{42}$$

On the other hand, the mass discharge rate at the sustainer phase ($\dot{m}_{d_S}$) is given by

$$\dot{m}_{d_S} = c_{D_S} A_t p \tag{46}$$

where c_{D_S} is determined using equation 20 adapted to the physical values of Propellant C. The mass balance is given by $\dot{m}_{d_s} = \dot{m}_{g_C}$ at the sustainer phase and is given by combining equations 42 and 46 as

$$c_{D_S} A_t p = a_C \rho_{p_C} p^{n_C} A_{b_C} \tag{47}$$

The equilibrium chamber pressure at the sustainer phase (p_{c_S}) is determined by the use of equation 24 as

$$p_{c_S} = \left(\frac{a_c \rho_{p_c} K_{n_S}}{c_{D_S}} \right)^{\frac{1}{1-n_c}} \tag{48}$$

where K_{n_S} is given by

$$K_{n_S} = \frac{A_{b_S}}{A_t} \tag{49}$$

The burning surface area at the sustainer phase $\left(A_{b_s}\right)$ becomes equivalent to the burning surface area of A_{b_C} after burnout of the booster phase.

9.3 Design of Propellant Grains

An example of a practical design requirement of thrust versus burn time is shown in Figure 16 for a two-stage motor composed of two grains in a single combustion chamber. The booster phase thrust (F_B) is 800 N and the burning time (t_{b_B}) is 1.0 s; the sustainer phase thrust (F_S) is 85 N and the burning time (t_{b_B}) is 27 s. The transient time of 0.3 s from the booster phase to the sustainer phase is included in the booster phase. Since the maximum chamber pressure is in the booster phase, the chamber pressure at the booster phase $\left(p_{c_B}\right)$ is chosen to be 11.0 MPa for the design booster pressure. This booster chamber pressure is assigned by the choice of the chamber wall thickness and the strength of the material.

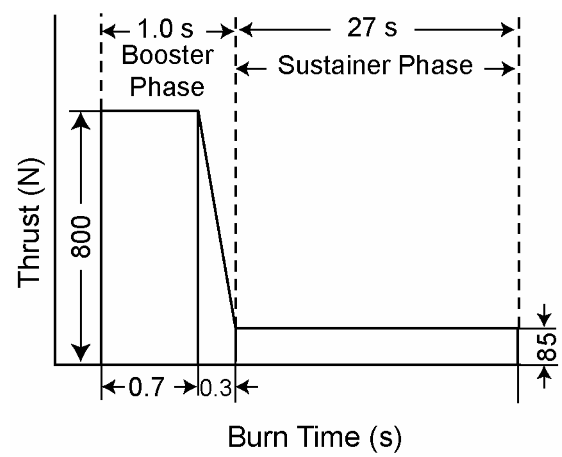

Figure 16. Thrust versus burning time requirement of a two-stage motor.

It is assumed that the convergent-divergent nozzle is designed to obtain an under expansion from p_{C_B} to atmospheric pressure p_a equal to 0.1 MPa. This is because the nozzle is used not only for the booster phase but also for the sustainer phase. Thus, the thrust coefficient c_{F_B} at the booster phase is determined to be 1.52 based on equation 29.

Using equation 28 one can get the nozzle throat area as

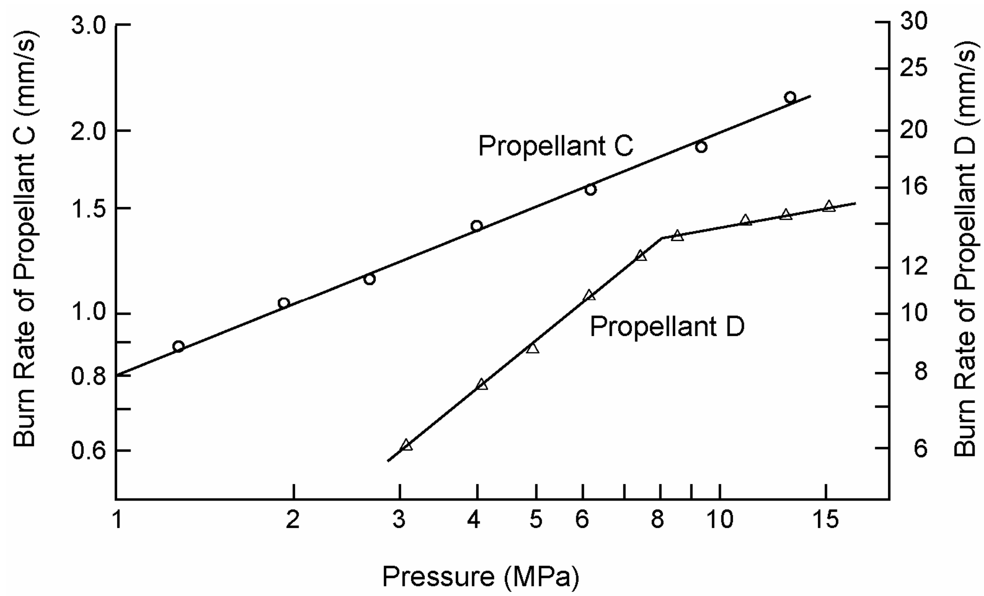

Figure 17. Burning rates of Propellant D and Propellant C as a function of pressure.

$$A_t = \frac{F}{c_{F_B} p_{c_B}} = \frac{800}{1.52 \times 11.0} = 47.8 \text{ mm}^2$$

The chamber pressure at the sustainer phase $\left(p_{c_S}\right)$ is also determined by the use of equation 28 as

$$p_{c_s} = \frac{F}{c_{F_s} A_t} = \frac{85}{1.30 \times 47.8} = 1.37 \text{ MPa}$$

where c_{F_S} is determined to be 1.30 because the nozzle expansion ratio is considered to be a close value of an optimum expansion of the nozzle.[11,12]

Accordingly, the design of the propellant grains used for the booster and sustainer phases is conducted at

p_{c_B} =11.0 MPa

p_{c_S} =1.37 MPa

A_t = 47.8 mm^2

The burn rate characteristics of Propellants D and C are shown in Figure 17. The physicochemical properties of the propellants are shown in Table 1.[11,12] The pressure exponent (n) of Propellant D changes from 0.81 below 8.0 MPa to 0.18 above 8.0 MPa. The burn rate

Table 1. Physicochemical Properties of Propellant D and Propellant C.

Property, Symbol (Units)	Propellant D		Propellant C
Density, ρ_p (kg/m^3)	1.57×10^{-3}		1.57×10^{-3}
Pressure exponent, n	$p \le 8.0$	0.81	0.40
	$p > 8.0$	0.18	
Burn rate constant, a	$p \le 8.0$	0.038	0.032
	$p > 8.0$	0.620	
Combustion temperature, T_g (K)	2470		1500
Gas constant, R_g (kg·m/kg·K)	36.9		33.9
Specific heat ratio, γ	1.25		1.24
Nozzle discharge coefficient, c_D (s^{-1})	7.38×10^{-3}		9.10×10^{-3}

(r) of Propellant C is extremely low to attain a low pressure burning and a long burning time (t_b). In addition, the combustion temperature (T_g) of Propellant C is low enough to protect against nozzle-throat erosion.

The burning area of the grain of Propellant C is determined by using equation 47 as

$$\begin{aligned} A_{b_C} &= \frac{c_{D_S} A_t}{a_C \rho_{p_C} p^{n_C - 1}} \\ &= \frac{9.10\times10^{-3}\times47.8}{0.032\times1.57\times10^{-3}\times1.37^{0.40-1}} \\ &= 4.20\times10^{4}\ \text{mm}^2 \end{aligned} \tag{50}$$

Using equations 41 to 45 plus combustion temperature, T_g, radius of curbature, R_g, and specific heat ratio, γ, obtained by NASA SP-273,[11] c_{D_B} and A_{b_D} are determined to be

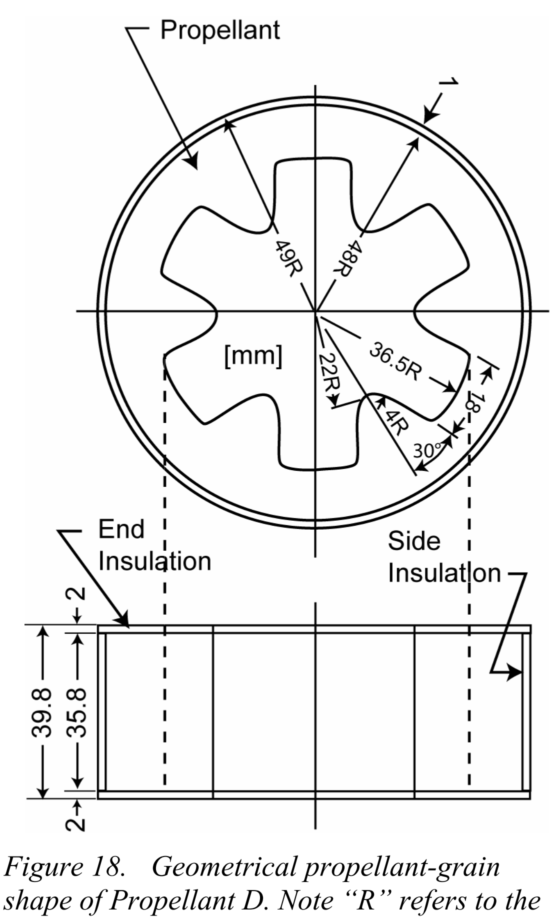

Figure 18. Geometrical propellant-grain shape of Propellant D. Note "R" refers to the radius of curvature.

$$c_{D_B} = 7.44\times10^{-3}\ \text{s}^{-1}$$

and the burning area of Propellant D is determined to be

$$A_{b_D} = 1.15\times10^{4}\ \text{mm}^2$$

Based on the required thrust versus burning time, the geometrical grain shapes are those shown in Figure 18 for Propellant D and in Figure 19 for Propellant C. The shape of the Propellant D grain is a wagon-wheel type, internal-burning shape, and the side and both ends are insulated with rubber sheets. The shape of the Propellant C grain is a star-type, internal and one-end burning shape, and the other end and the perimeter are insulated with rubber sheets. The relationship between the burning area and the regressing grain from the initial

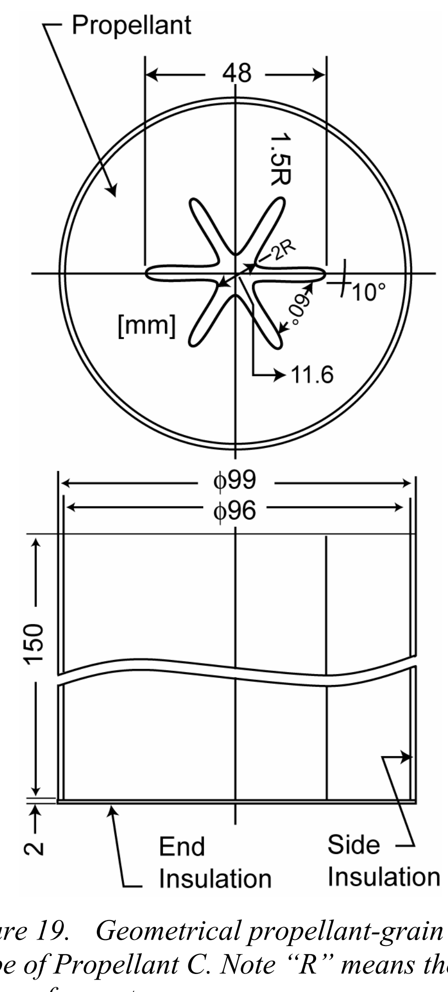

Figure 19. Geometrical propellant-grain shape of Propellant C. Note "R" means the radius of curvature.

surface is shown in Figure 20 for both Propellant D and Propellant C grains.

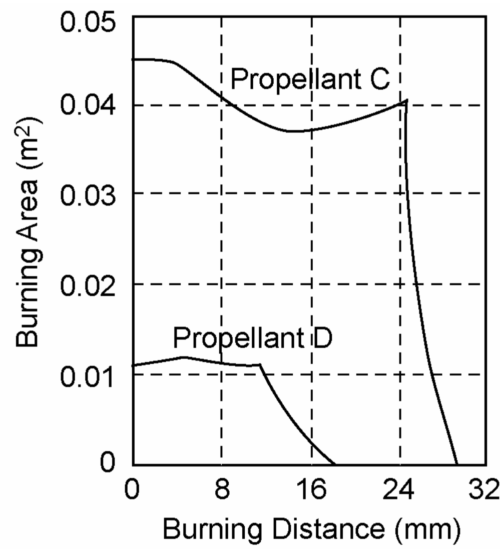

Figure 20. Relationship of burning area and regressing grain distance (web thickness consumed) of Propellant D and Propellant C.

9.4 Firing Test Results

Both grains, Propellants D and C, are set in a heavy weight rocket motor for static firing tests as shown in Figure 21. A pyrotechnic igniter, which is ignited electrically, is attached at the head end of the rocket motor, and a convergent-divergent nozzle is attached at the rear end of the motor. Pressure in the motor is measured with a pressure transducer gauge attached to the head end of the motor. Thrust is measured with a load-cell set in the thrust bench on which the rocket motor is set.

Figure 22 shows a pressure versus burning time curve of the rocket motor shown in Figure 21. The experimental curve agrees with the theoretical curve except for the increased pressure of 1.8 MPa at the booster phase. The burning time of the sustainer phase decreased about 0.6 s due to the excess burning of Propellant C during the booster phase. This observed excess burning of Propellant C during the booster phase is considered to be an effect of erosive burning, which occurs during high cross flow along the burning surface of Propellant C.

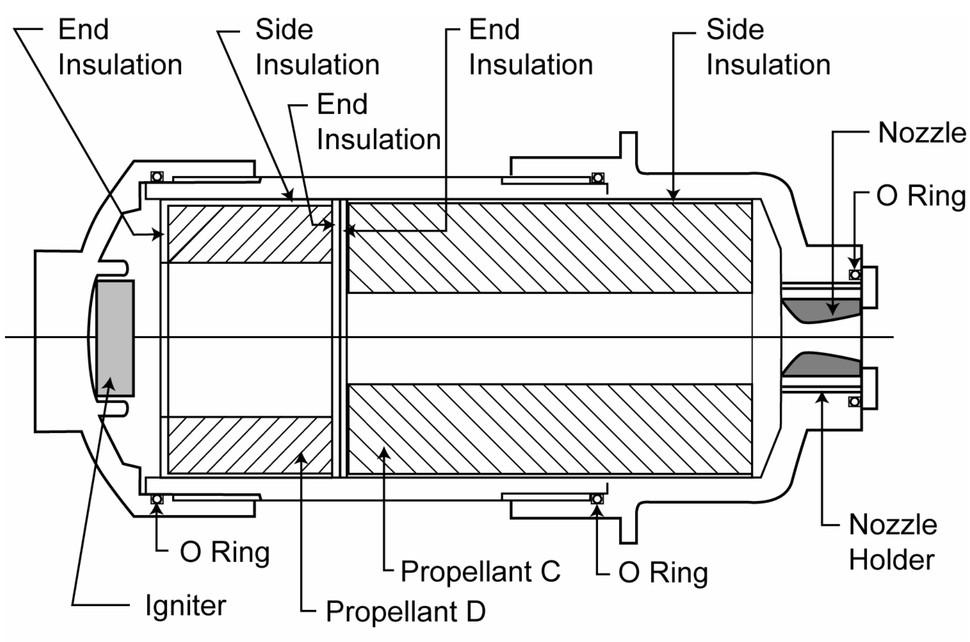

Figure 21. A structure of the two-stage heavy-weight motor with Propellant D and Propellant C grains in a single chamber.

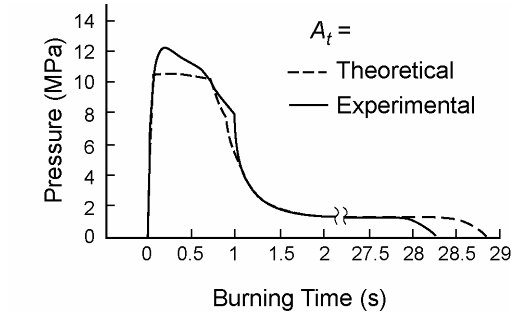

Figure 22. Theoretical and experimental results of pressure versus burning time of the two-stage motor with two propellant grains in one single chamber shown in Figure 21.

To examine the erosive burning effect on the burning rate of Propellant C, a burning interruption experiment was performed. One second after ignition of the rocket motor, the nozzle attached at the end of the rocket motor was separated. The chamber pressure decreased rapidly to atmospheric pressure (0.1 MPa). The Propellant D grain was completely consumed, but Propellant C grain remained. Figure 23 shows the cross-sectional star shaped Propellant C grain before combustion (a) and after it was extinguished (b) at the time of the Propellant D burnout. These results indicate that the burning rate of Propellant C increased about 7 % due to the erosive burning effect. This is confirmed by the pressure versus time plot shown in Figure 22.

Summary

The performance of a rocket motor is dependent on the physicochemical parameters of propellants such as burning rate, pressure exponent, temperature sensitivity, and the physical shape of the propellant grain. The thrust required for the rocket motor is determined by the required flight trajectory and by the aerodynamic drag that acts on the rocket projectile.

The thrust is dependent on the combustion pressure and the nozzle throat area that are determined by the mass generation rate and the mass discharge rate. A two-stage- rocket motor is attained by the combination of two different types of propellant grains in the combustion chamber.

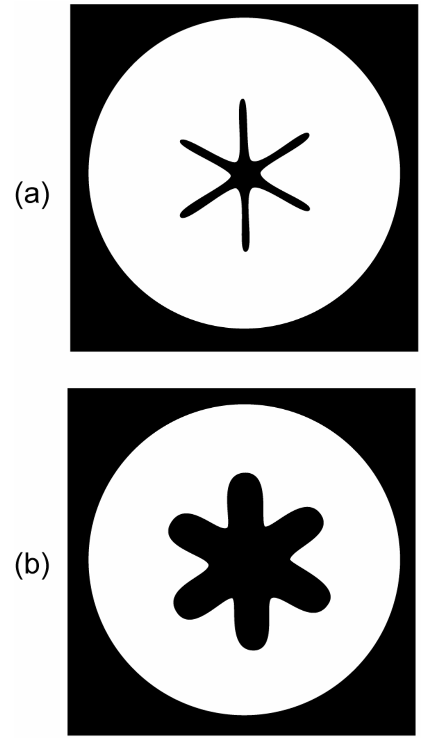

Figure 23. Cross-sectional star-shaped grain of Propellant C before combustion (a) and after being extinguished (b) one second into the burn.

References

1) N. Kubota, *Rocket Combustion*, Nikkan Kogyo Press, Tokyo, 1995.

2) N. Kubota, *Propellants and Explosives*, Wiley-VCH, Weinheim, 2002.

3) G. P. Sutton, *Rocket Propulsion Elements*, 6^{th} ed., John Wiley & Sons, New York, 1992.

4) N. Kubota, "Survey of Rocket Propellants and their Combustion Characteristics, Fundamentals of Solid-Propellant Combustion", eds. K. K. Kuo and M. Summerfield, *Progress in Astronautics and Aeronautics*, Vol. 90, Chapter 1, AIAA, New York, 1984.

5) N. Kubota, "Temperature Sensitivity of Solid Propellants and Affecting Factors: Experimental Results, Nonsteady Burning and Combustion Stability of Solid Propel-

lants", eds. L. DeLuca, E. W. Price, and M. Summerfield, *Progress in Astronautics and Aeronautics*, Vol. 143, Chapter 4, AIAA, New York, 1990.

6) N. Kubota, "Propellant Chemistry", *Journal of Pyrotechnics*, Issue 11, 2000, pp 25–45.

7) A. Davenas, *Solid Rocket Propulsion Technology*, Pergamon Press, New York, 1993.

8) Y. M. Timnat, *Advanced Chemical Rocket Propulsion*, Academic Press, New York, 1987.

9) T. Niioka, T. Mitani, and S., Ishii, "Transient Period of the Acceleration-Produced Burning Rate Augmentation", *AIAA Journal*, Vol. 14, No. 9, 1976, pp 1165–1169.

10) T. Mitani and T. Niioka, "An Analytical Model of Solid Propellant Combustion in an Acceleration Field", *Combustion Science and Technology*, Vol. 15, 1977, pp 107–114.

11) S. Gordon, and B. J. McBridge, *Computer Program for Calculation of Complex Chemical Equilibrium Compositions, Rocket Performance, Incident and Reflected Shocks, and Chapman-Jouguet Detonations*, NASA SP-273, 1971.

12) *JANAF Thermochemical Tables*, Dow Chemical Co., Midland, MI, USA (1960–1970).